Check for updates

Radio Science

RESEARCH ARTICLE
10.1029/2020RS007258

Ionospheric Echo Detection in Digital Ionograms Using Convolutional Neural Networks

C. De La Jara[1] and C. Olivares[2]

[1]Instituto Geofísico del Perú, Lima, Peru, [2]Pontificia Universidad Católica del Perú, Lima, Peru

Key Points:

- This is the first time a multilayer convolutional neural network has been used to identify ionogram traces
- The trace extraction performance of the neural network surpasses the performance of some machine learning models. A comparison is presented
- The NN presented does not need a large amount of unlabeled data, good performance is achieved using a small number of labeled data

Supporting Information:

Supporting Information may be found in the online version of this article.

Correspondence to:

C. De La Jara,
delajara.c@gmail.com

Citation:

De La Jara, C., & Olivares, C. (2021). Ionospheric echo detection in digital ionograms using convolutional neural networks. *Radio Science*, *56*, e2020RS007258. https://doi.org/10.1029/2020RS007258

Received 7 JAN 2021
Accepted 20 JUL 2021

© 2021. American Geophysical Union. All Rights Reserved.

Abstract An ionogram is a graph of the time that a vertically transmitted wave takes to return to the earth as a function of frequency. Time is typically represented as virtual height, which is the time divided by the speed of light. The ionogram is shaped by making a trace of this height against the frequency of the transmitted wave. Along with the echoes of the ionosphere, ionograms usually contain a large amount of noise and interference of different nature that must be removed in order to extract useful information. In the present work, we propose a method based on convolutional neural networks to extract ionospheric echoes from digital ionograms. Extraction using the CNN model is compared with extraction using machine learning techniques. From the extracted traces, ionospheric parameters can be determined and electron density profile can be derived.

1. Introduction

Ionosondes are a type of radar that send pulses of high frequency radio waves to the ionosphere in the vertical direction. The echoes of these pulses are recorded on the ground and are used to generate a type of representative traces of the ionosphere, called ionograms, which are a representation of the state of the ionosphere at a given time. There is a direct relation between the frequency of the transmitted pulses and the ionization densities of the ionospheric layers that reflect them (Piggot & Rawer, 1972).

Figure 1 shows an example of a typical ionogram. Horizontal axis represents the frequencies of the transmitted radio signals and the vertical axis the virtual heights of ionospheric layers. The color of the trace is proportional to the intensity of the received signal, more intense echoes will have colors closer to red, while weaker echoes to blue. In this image it can also be clearly distinguished as F1 layers over a height of 200 km and F2 over 300 km.

Echoes form characteristic patterns, which comprise an ionogram. Critical frequencies are the limiting frequencies at which a wave is reflected by an ionospheric layer. Waves of frequencies above them penetrate through the layers. From ionograms it is possible to scale, manually or by computational methods, characteristic values of virtual heights h'E, h'F, h'F2, etc and critical frequencies foE, foF1, foF2, etc of each layer of the ionosphere (Perrone et al., 2017). In addition, the speed of the pulses traveling in the ionosphere is lower than the speed of the pulses traveling in free space. Therefore, it is possible to obtain information about the electron densities in the ionosphere by building a profile from the bottom up. This process will require some assumptions about the nature of the layers such as the existence and depth of any areas where the electron density decreases with altitude and which therefore cannot be probed by an ionosonde.

Interest in scaling and interpreting ionograms is increasing among the scientific community. Extracting ionospheric parameters by manual scaling is a very demanding task, both in effort and time. With the development of image processing techniques, advances have been made in the process of automatic scaling ionograms.

ARTIST is one of the most widely used methods for automatic ionogram scaling in real time (Galkin and Reinisch, 2008). Chen proposed an algorithm for automatic scaling ionograms using an image recognition technique (Chen et al., 2018). Pezzopane and Scotto developed methods for automatic scaling of F1 (Pezzopane et al., 2008), foF2 and MUF (2000) (Scotto & Pezzopane, 2002), and sporadic E layers (Pezzopane & Scotto, 2007) Harris developed methods to separate O and X modes (Harris et al., 2017) (Harris & Pederick, 2017). Ding developed a method to scale F2 parameters using orthogonal function and image processing (Ding et al., 2007).

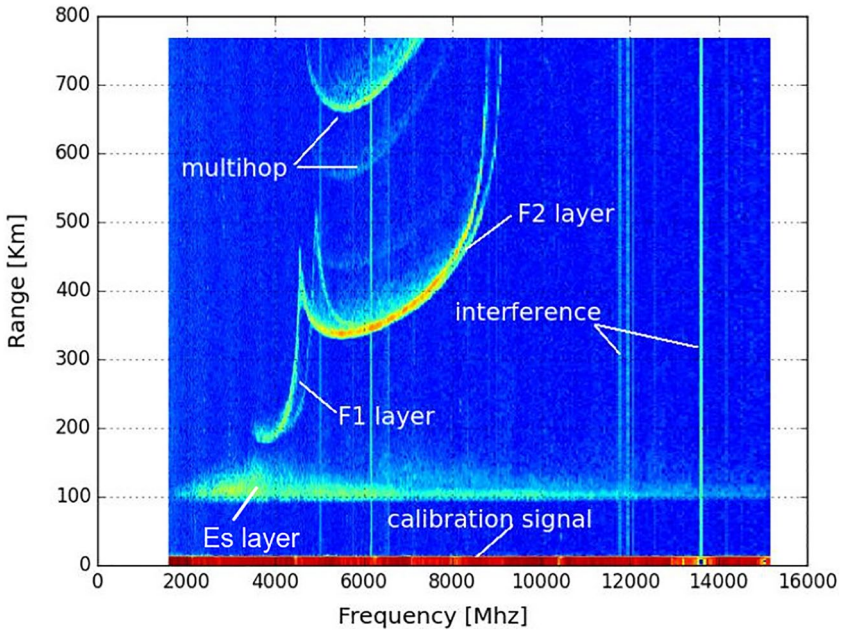

Figure 1. Ionogram of Jicamarca ionosonde showing the virtual ionospheric height (vertical) versus frequency of transmitted pulses (horizontal). The traces show F1 and F2 layers as well as multihop, interference, and calibration signal.

Emphasis is usually placed on the recognition of ionogram traces, to later obtain the density profiles by applying ionospheric inversion techniques. In highly complex situations, such as incomplete ionograms or ionograms with the presence of phenomena such as spread F, automatic scaling becomes more difficult and tends to fail (Stankov et al., 2012).

In the present work, we propose the use of a convolutional neuronal network model for the detection of ionosphere echoes in digital ionograms, which can serve as a tool for automatic scaling. This work represents the first step in the development of a system for near-real time, automatic and accurate scaling of ionograms generated by ionosondes of the The Low Latitude Ionospheric Sensor Network (LISN) observatory (Figure 2) using neural networks, so characteristic values of ionospheric regions, such as critical frequencies, can be obtained. Due to the large amount of data generated by the network, it is not possible to consider using manual scaling in a regular basis, but this large amount of data can be used to train a deep learning network, which have a powerful ability to manage large amounts of data (Xiao et al., 2020).

The work is structured as follows: Section 2 gives a brief introduction to the operation mode of ionosondes, as well as characteristics of the ionosphere. Section 3 describes the characteristics of the data set used, how it was obtained and what preprocessing was done. Section 4 describes the performance metric to be used. Section 5 describes and evaluates the performance of the baseline models. Section 6 describes the use of convolutional neural networks for profile detection.

2. The Ionosphere

The ionosphere is a part of the earth's upper atmosphere, extending in height from 60 to about 1,000 km. This region is composed of ionized gas, called plasma. The upper limit of the ionosphere is defined as the height at which the concentration of charged particles of plasma, ions, and electrons, exceed the concentration of neutral atoms and molecules. At this point the ionosphere begins to continuously transform into the magnetosphere, which it is a medium consisting only of strongly ionized plasma and intense electric and magnetic fields.

The ionosphere is formed when incident solar radiation removes electrons from gases of the upper atmosphere, creating electrically charged ions and free electrons. The ionization becomes greater when high

1944799x, 2021, 8, Downloaded from https://agupubs.onlinelibrary.wiley.com/doi/10.1029/2020RS007258 by Cochrane Peru, Wiley Online Library on [19/08/2025]. See the Terms and Conditions (https://onlinelibrary.wiley.com/terms-and-conditions) on Wiley Online Library for rules of use; OA articles are governed by the applicable Creative Commons License

Figure 2. The dots represent the geographic distribution of the ionosondes of the LISN distributed observatory, nearly aligned with the magnetic flux tube intersecting the magnetic equator at 70 deg West.

energy radiation interacts with a greater density of air, and decreases when radiation loses intensity as it travels down the atmosphere.

Usually the ionosphere is divided into five independent regions, called layers. The lower layer, which ranges from 70 to 90 km in height, is called layer D; from 95 to 140 km is layer E, and above 140 km is layer F. The latter is usually divided into two regions, F1, ranging from 140 to 200 km, and layer F2, which is above 200 km (Jursa, 1985).

3. Data Set Description

The data used for the training of the convolutional networks and the evaluation of the baseline models were obtained from the database of the distributed observatory LISN (Observatorio distribuido lisn, 2019), which is a multi-institution, multi-instrument project in which a set of geophysical observation instruments have

19447994x, 2021, 8, Downloaded from https://agupubs.onlinelibrary.wiley.com/doi/10.1029/2020RS007258 by Cochrane Peru, Wiley Online Library on [19/08/2025]. See the Terms and Conditions (https://onlinelibrary.wiley.com/terms-and-conditions) on Wiley Online Library for rules of use; OA articles are governed by the applicable Creative Commons License

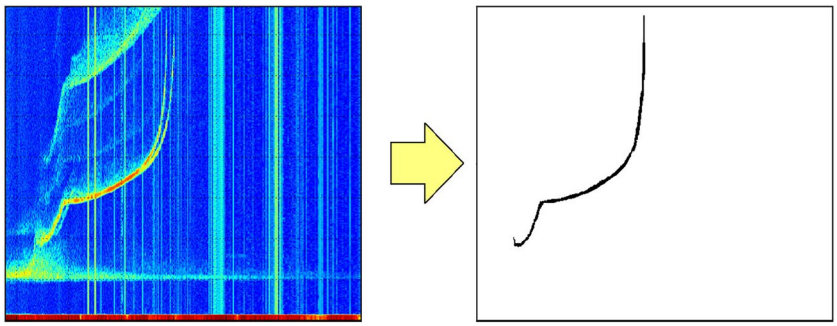

Figure 3. Ionogram before and after been manually converted to a binary image.

been deployed in different locations in South America in order to study the electrodynamics of the ionosphere, with emphasis on the dynamic energy transport and photo chemical processes, and also to develop the ability of predicting spread F occurrence and measurement of plasma densities, drifts, and neutral winds in a large geographic area (Valladares & Chau, 2012).

Among the instruments used in the project there are 4 VIPIR ionosondes, in the cities of Lima and Puerto Maldonado in Peru, Tupiza in Bolivia and Tucuman in Argentina, whose ionograms will make up the data set. The data generated by these instruments have two objectives: education and scientific research, they are freely available (lisn data user rules, 2019) and can be downloaded from the project website.

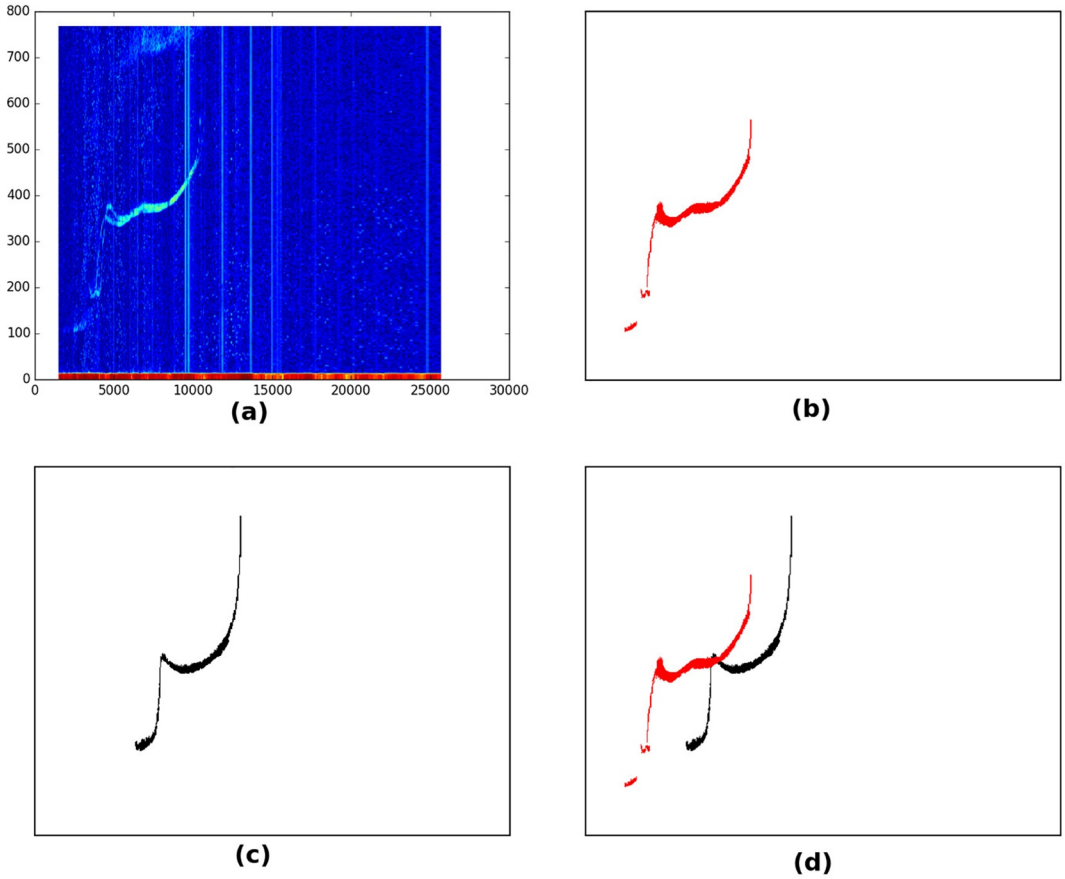

Figure 4. (a) Original ionogram, (b) Manual extraction, (c) Automatic extraction, (d) Comparison between manual and automatic extraction.

1944799x, 2021, 8, Downloaded from https://agupubs.onlinelibrary.wiley.com/doi/10.1029/2020RS007258 by Cochrane Peru, Wiley Online Library on [19/08/2025]. See the Terms and Conditions (https://onlinelibrary.wiley.com/terms-and-conditions) on Wiley Online Library for rules of use; OA articles are governed by the applicable Creative Commons License

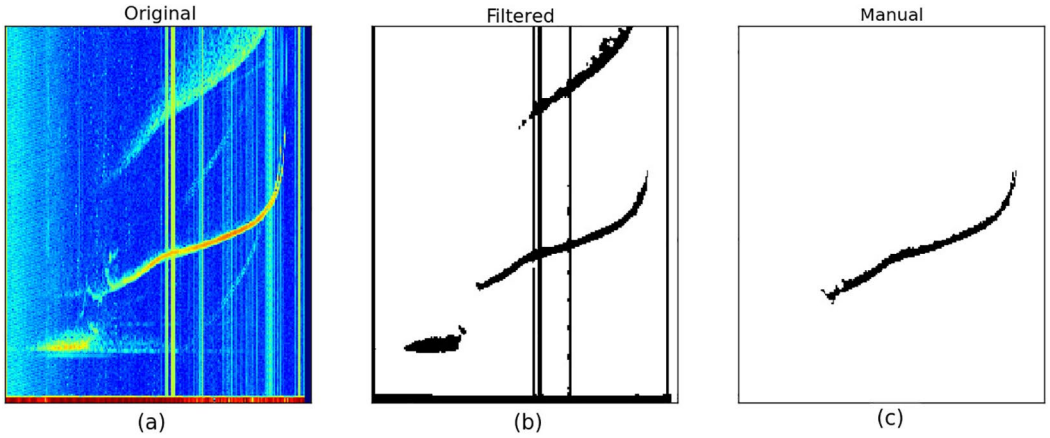

Figure 5. (a) Comparison between the original ionogram , (b) the result of the cascade application of the K filter, median filter and thresholding, and(c) a manual trace extraction.

The data output of the VIPIR ionosondes is a Raw In-phase and Quadrature (RIQ) file that contains a number of range gate samples of the output of the Digital Down Converter for each of the eight radar receive channels. These define the instrument mode of operation and the site-specific information such as station location and antenna configuration. RIQ files are binary files with a specific, custom format (Bullet, 2015). RIQ FILES are converted and stored in NetCDF (ngi) format (Network common data form, 2019). Ngi files store the required information to decode and plot ionograms, such as radar configuration, pulse configuration table, and IQ data blocks.

The LISN database contains more than 900,000 ionograms. Depending on the geographical location and the type of experiment performed, the configuration of the ionosondes may vary, so the number of frequency and height points is not constant throughout the database. A group of 50,780 ionograms from the Jicamarca station was chosen to train the model. These ionograms were taken between 15:00 and 22:00 h GMT from years 2016–2018. All of the ionograms chosen have a height of 512 and 408 frequency points. From this set, 816 were randomly selected to manually extract ionosphere profiles (we call this manual extraction), and these files made up the labeled data set.

Figure 3 shows an ionogram before and after being manually converted to a binary image, in which the ionosphere profile has been extracted.

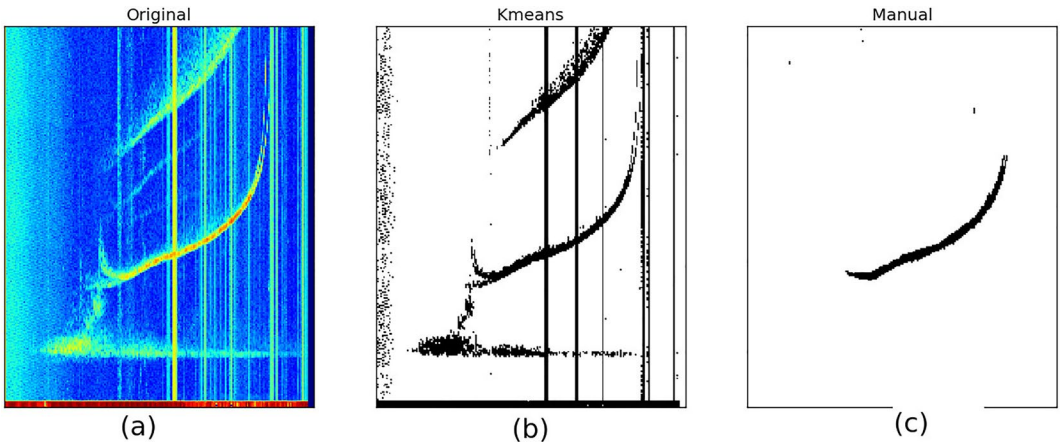

Figure 6. (a) Comparison between the original ionogram, (b) application of K- menas, (c) and manual trace extraction.

1944799x, 2021, 8, Downloaded from https://agupubs.onlinelibrary.wiley.com/doi/10.1029/2020RS007258 by Cochrane Peru, Wiley Online Library on [19/08/2025]. See the Terms and Conditions (https://onlinelibrary.wiley.com/terms-and-conditions) on Wiley Online Library for rules of use; OA articles are governed by the applicable Creative Commons License

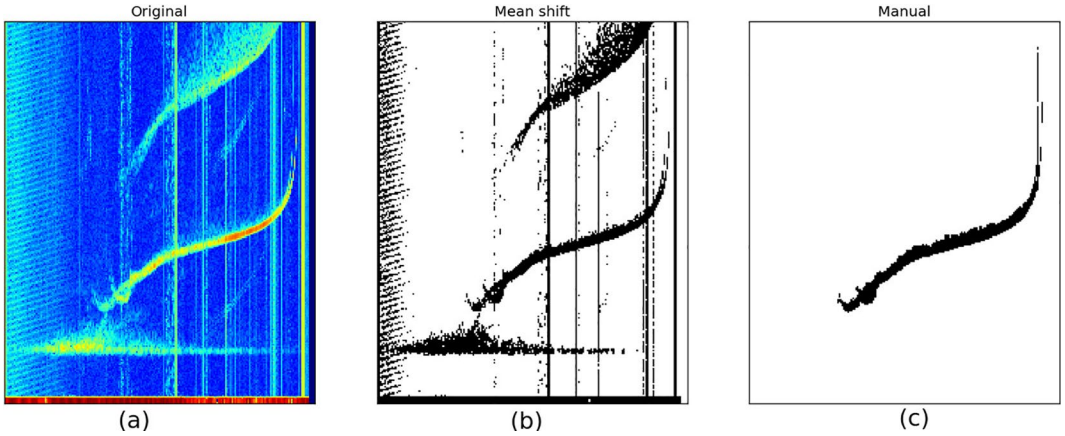

Figure 7. (a) Comparison between the original ionogram, (b) application of mean shift and, (c) manual trace extraction.

4. Performance Metrics

In this work, we propose a method to extract ionospheric layers from digital ionograms using image segmentation with convolutional neural networks, where the main goal is to label every pixel of the image as belonging to the ionosphere trace or belonging to the background.

The most common performance metrics used for object segmentation problems is an index called intersection over union (IoU) (Rahman & Wang, 2016) (Mochalov & Mochalova, 2019). IoU gives a ratio between the number of pixels common in two images and the total number of pixels in both images. If the images are exactly the same, the result of this ratio would be one, if there were few coincidences between the images (very different images), the result would be close to 0.

$$IoU = \frac{common\ area}{total\ area} \tag{1}$$

Since we are working with binary matrices the area is obtained by making a sum of all the cells in the matrix. The intersection will be obtained by performing a logical AND operation between the bits of the matrices and the union will be obtained by performing a logical OR.

Figure 4 shows a concept of the technique that will be used to compare manual and automatic extraction (no segmentation technique was used to generate these traces). Manually extracted traces (b) will be compared with automatic extracted traces (c) using IoU. In this example, at the pixel level, the intersection matrix (d) will have only a few elements in one, resulting in an IoU close to zero. Manual extraction is considered to be perfect.

5. Implementation and Evaluation of Baseline Models

5.1. Profile Detection Using Image Processing and Thresholding

In this approach, ionograms are considered as images, in which noise and interference must be filtered out to isolate ionospheric echoes. For this purpose, original ionograms are passed through three filters:

1. Median filter
2. Thresholding.
3. The filter defined by the matrix K.

Table 1
Baseline Models Average IOU

	Filtered	K-means	Mean shift
IoU	0.163	0.157	0.105

Abbreviation: IoU, intersection over union.

$$K = \begin{matrix} 1 & 1 & 1 & 0 & 1 & 1 & 1 \\ 1 & 1 & 1 & 0 & 1 & 1 & 1 \\ 1 & 1 & 1 & 0 & 1 & 1 & 1 \\ 1 & 1 & 1 & 0 & 1 & 1 & 1 \\ 1 & 1 & 1 & 0 & 1 & 1 & 1 \\ 1 & 1 & 1 & 0 & 1 & 1 & 1 \end{matrix} \tag{2}$$

1944799x, 2021, 8, Downloaded from https://agupubs.onlinelibrary.wiley.com/doi/10.1029/2020RS007258 by Cochrane Peru, Wiley Online Library on [19/08/2025]. See the Terms and Conditions (https://onlinelibrary.wiley.com/terms-and-conditions) on Wiley Online Library for rules of use; OA articles are governed by the applicable Creative Commons License

Layer (type)	Output Shape	Param #
input_3 (InputLayer)	(None, 256, 208, 1)	0
conv2d_15 (Conv2D)	(None, 256, 208, 16)	160
max_pooling2d_7 (MaxPooling2	(None, 128, 104, 16)	0
conv2d_16 (Conv2D)	(None, 128, 104, 8)	1160
max_pooling2d_8 (MaxPooling2	(None, 64, 52, 8)	0
conv2d_17 (Conv2D)	(None, 64, 52, 8)	584
max_pooling2d_9 (MaxPooling2	(None, 32, 26, 8)	0
conv2d_18 (Conv2D)	(None, 32, 26, 8)	584
up_sampling2d_7 (UpSampling2	(None, 64, 52, 8)	0
conv2d_19 (Conv2D)	(None, 64, 52, 8)	584
up_sampling2d_8 (UpSampling2	(None, 128, 104, 8)	0
conv2d_20 (Conv2D)	(None, 128, 104, 16)	1168
up_sampling2d_9 (UpSampling2	(None, 256, 208, 16)	0
conv2d_21 (Conv2D)	(None, 256, 208, 1)	145

Total params: 4,385
Trainable params: 4,385
Non-trainable params: 0

Figure 8. Neural network model.

As shown in Figure 5, after passing through the three filters it is possible to accurately eliminate the background noise from ionograms, but neither the interference, nor the calibration signal nor multihop can be eliminated.

Average IoU between ionograms where the three filters were applied and manual trace extraction is 0.163.

5.2. Profile Detection Using Unsupervised Machine Learning Models

The other method is based on the representation of the ionograms in 3-dimensional matrices {x, y, V} where x and y represent spatial coordinates and V the intensity of the point. With this representation two unsupervised clustering techniques are applied, K-Means and Mean Shift.

Clustering is a grouping technique to find, within a set of samples, groups that have similar characteristics, so samples that share comparable features will belong to the same group, and will be separated from other groups. The goal is to maximize variations between groups and minimize variations inside groups (Pham et al., 1989-1996).

K-means clustering: K-means is a nonsupervised learning clustering technique that searches patterns in the data without having a specific prediction as a goal. K-means needs as input the number of groups (k) in which the samples will be segmented. Knowing this, the algorithm places k random points as center of clusters, then assigns to this points the samples with the shortest distances. The point then shifts in the direction of the closest average distance and this process is repeated iteratively and the groups are adjusted until the centroid does not change further by moving the points. One of the K-means algorithm drawbacks is that it requires the number of clusters to be specified before the algorithm is applied. In this work, we consider that a number of clusters equal to two reflects a specific characteristic of the data set, since we want to cluster the ionogram points into two main classes, ionospheric echoes and background noise. Figure 6 shows a comparison between an original ionogram, trace extraction using K-means, and a manual trace extraction. As with the application of the filters, interference, multihop, and calibration signals are not removed.

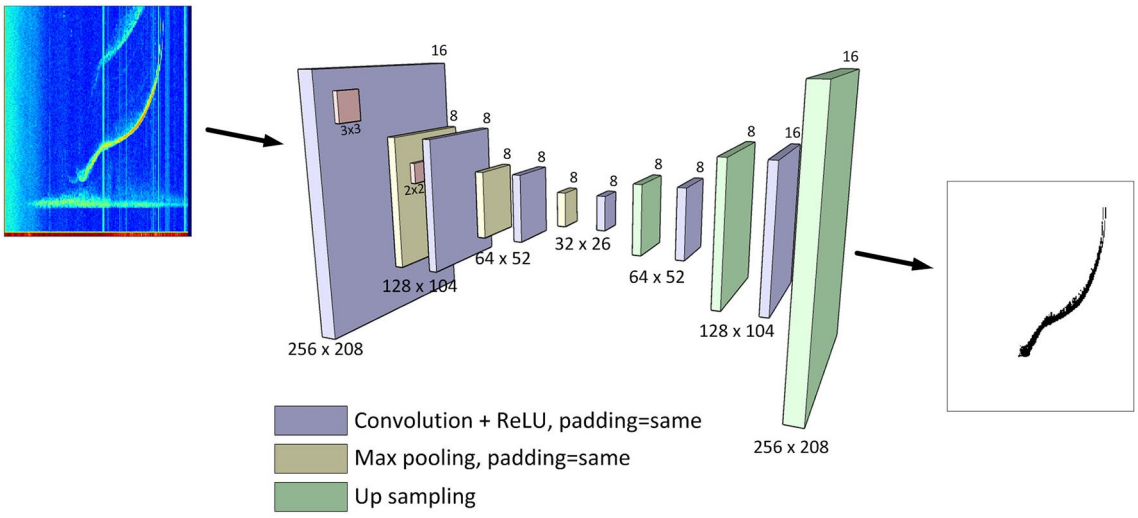

Figure 9. Layers of the neural network model.

19447994x, 2021, 8, Downloaded from https://agupubs.onlinelibrary.wiley.com/doi/10.1029/2020RS007258 by Cochrane Peru, Wiley Online Library on [19/08/2025]. See the Terms and Conditions (https://onlinelibrary.wiley.com/terms-and-conditions) on Wiley Online Library for rules of use; OA articles are governed by the applicable Creative Commons License

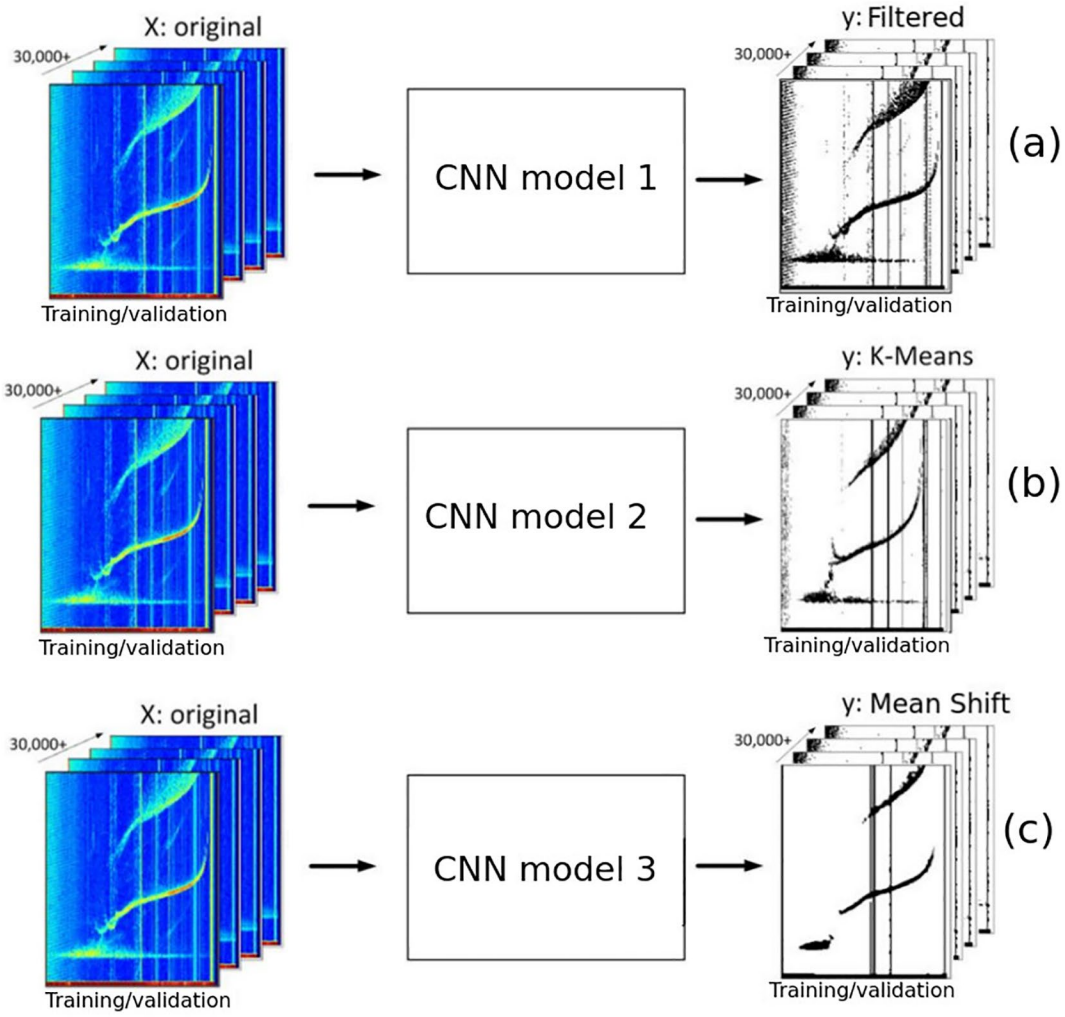

Figure 10. Input data of all models are original ionograms. (a) CNN model 1: output variables are ionograms with traces extracted using filters. (b) CNN model 2: output variables are ionograms with traces extracted using K-means. (c) CNN model 3: output variables are ionograms with traces extracted using mean shift.

Average IoU between trace extraction using K-means and manual extraction, for the test set is 0.157.

Mean shift clustering: Mean shift is also a nonsupervised learning clustering technique that assigns the samples to the clusters by moving the center of these toward the direction of highest density of samples (Cheng, 1995). Given a data set, mean shift is the displacement of a point from an initial location in the space, to another that results from the average of the weights of the data within a neighborhood determined by a region centered in x. Unlike K-Means algorithm, mean shift does not require a previous knowledge of the number of clusters; they are determined by the algorithm with respect to the data.

Figure 7 shows a comparison between an original ionogram, trace extraction using mean shift and manual extraction.

Average IoU between trace extraction using mean shift and manual extraction for the test set is 0.105

Table 1 summarizes the results of the IoU for the three baseline models.

1944799x, 2021, 8, Downloaded from https://agupubs.onlinelibrary.wiley.com/doi/10.1029/2020RS007258 by Cochrane Peru, Wiley Online Library on [19/08/2025]. See the Terms and Conditions (https://onlinelibrary.wiley.com/terms-and-conditions) on Wiley Online Library for rules of use; OA articles are governed by the applicable Creative Commons License

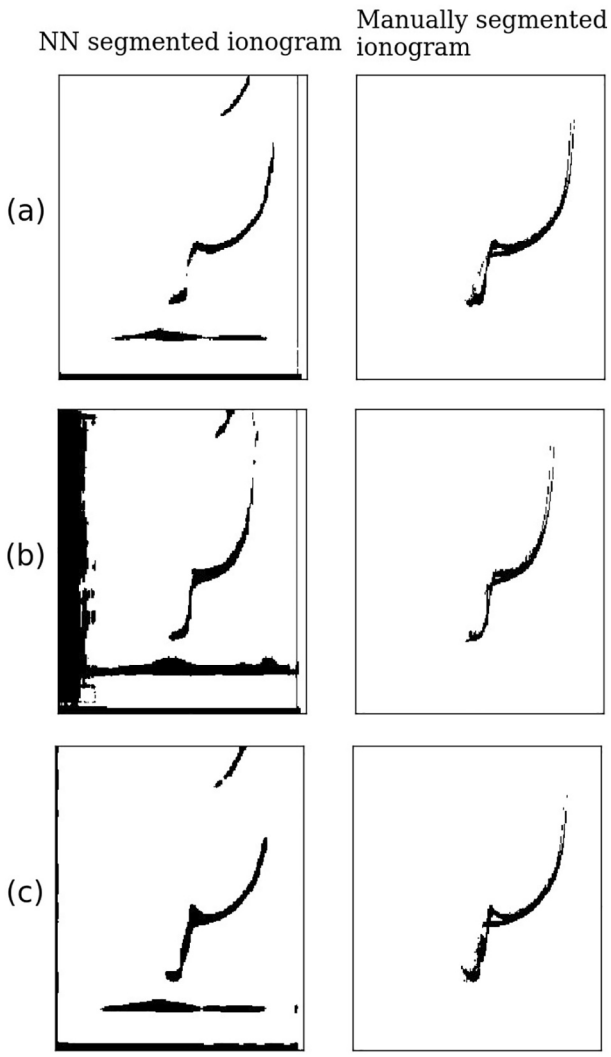

Figure 11. Baseline model learning. Left column is the reconstruction of an ionogram using a neural network model trained with a base ine model, and the right column is the manual trace extraction. (a) Kmeans, (b) Mean shift (c) filters.

Table 2
Convolutional Network Average IOU

	Filtered	K-means	Mean shift
IoU	0.174	0.173	0.077

Abbreviation: IoU, intersection over union.

6. Profiles Detection Using Convolutional Neural Networks

A large amount of unlabeled data is available from the LISN database, on the other hand, labeled data can only be obtained by performing manual trace extraction of ionograms, which is not only a time consuming process but also requires a high level of knowledge and experience. Given this scenario, with the goal of building a semisupervised learning model, both types of data have been used, the large amount of unlabeled data and the small number of labeled (manually extracted) ionograms.

We used a model based on a multilayer convolutional encoder decoder neural network, with multiple layers of convolutions (Alexandre et al., 2018). The model architecture has some similarities with an autoencoder, in the sense that it is also used for the task of representation learning, and is used to reconstruct data, but is not exactly the same, given that the input and output of the network are not intended to be the same. The first part of the network is an encoder that maps raw inputs to a rich representation of feature vectors, the second part is a decoder that takes this feature representation as input, process it, produces an output, and maps the output back into the raw format. The network goal is to learn an efficient representation of the data.

Figure 8 shows a description of the network model.

Input image size: 256 × 208

Encoder:
- Convolution layers: 3
  - filters: 16, 8, 8
  - kernel sizes: 3, 3, 3
  - activation: ReLU
  - Padding: same
- max pooling layers: 3
  - kernel sizes: 2, 2, 2
  - Padding: same

Decoder:
- Convolution layers: 3
  - filters: 8, 8, 16
  - kernel sizes: 3, 3, 3
  - activation: ReLU
  - padding: same
- Up sampling layers: 3
  - kernel sizes: 2, 2, 2
  - padding: same

Optimizer: Adadelta

Loss function: binary cross entropy

Figure 9 shows details of the different layers of the neural network model.

The training set used has 31,699 ionograms, the validation set 9,577, and the test set 9,505. Eight hundred sixteen ionograms were manually scaled, from them 474 are used as training set, 151 as validation set, and 191 as test set. The process was divided in three stages, in the first stage 31,699 original ionograms were used to train a model, in the second stage the 474 manually extracted traces were used to fine-tune the pretrained

1944799x, 2021, 8, Downloaded from https://agupubs.onlinelibrary.wiley.com/doi/10.1029/2020RS007258 by Cochrane Peru, Wiley Online Library on [19/08/2025]. See the Terms and Conditions (https://onlinelibrary.wiley.com/terms-and-conditions) on Wiley Online Library for rules of use; OA articles are governed by the applicable Creative Commons License

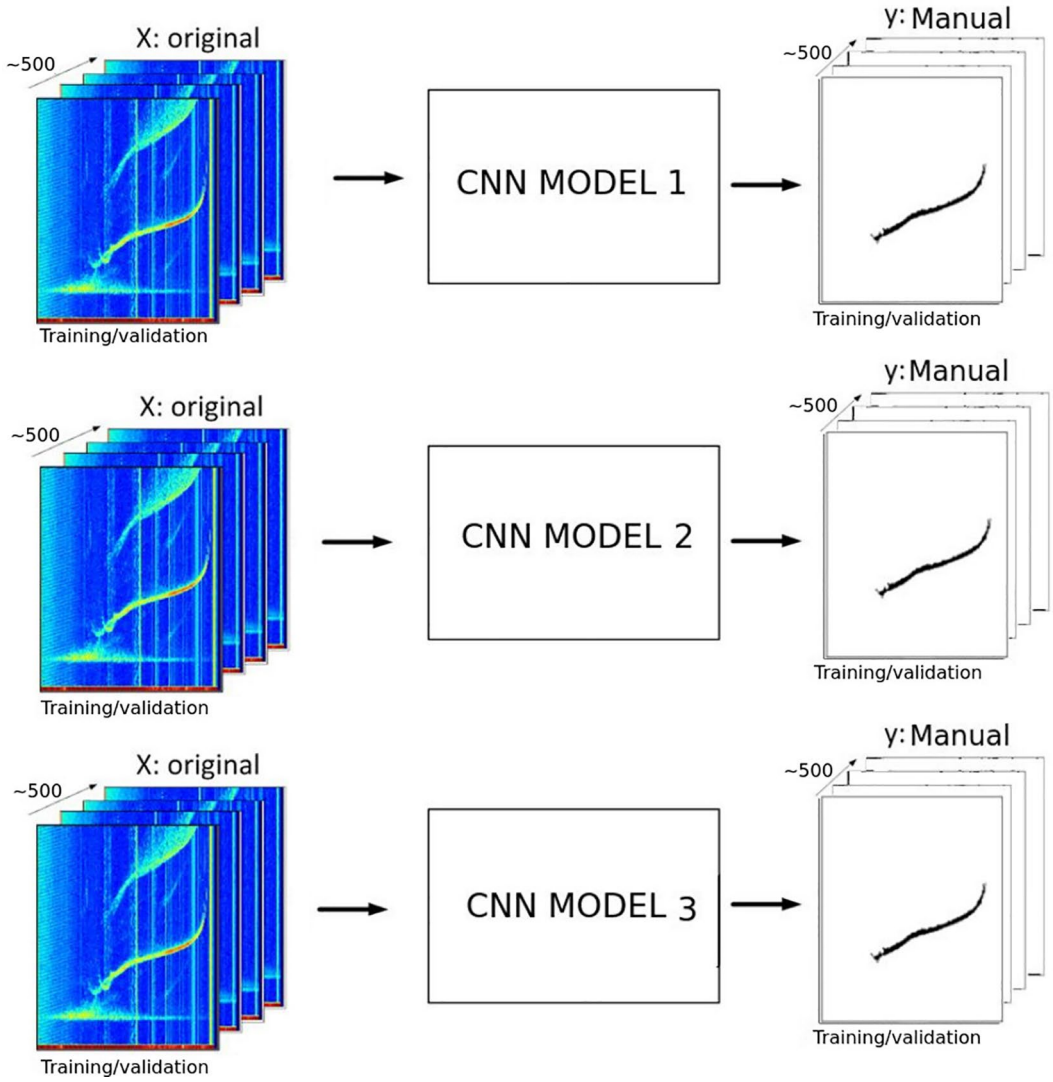

Figure 12. Fine-tuning of pretrained models. Input data of all models are original ionograms and output variables are ionograms with manually extracted traces.

model from the first stage, and in the last stage a new model is trained using only manually extracted traces. The results of these two models are compared.

6.1. Pretraining: Building a Neural Network Model From Baseline Models

In the first stage of the learning process, we feed the neural network with original ionograms (X) from the training/validation sets, and use as output variables (y) ionograms with traces extracted using the three baseline techniques (filters, k-means and mean shift). We end up with three neural network models, each one learned to reconstruct ionograms the same way baseline models do it, as shown in Figure 10.

The application of each of these models in the test set compared to manual trace extraction is shown in Figure 11

Average IoU between ionograms with traces extracted with these CNN models and manual extraction is summarized in Table 2. A small improvement is observed compared to the IoU of baseline models.

1944799x, 2021, 8, Downloaded from https://agupubs.onlinelibrary.wiley.com/doi/10.1029/2020RS007258 by Cochrane Peru, Wiley Online Library on [19/08/2025]. See the Terms and Conditions (https://onlinelibrary.wiley.com/terms-and-conditions) on Wiley Online Library for rules of use; OA articles are governed by the applicable Creative Commons License

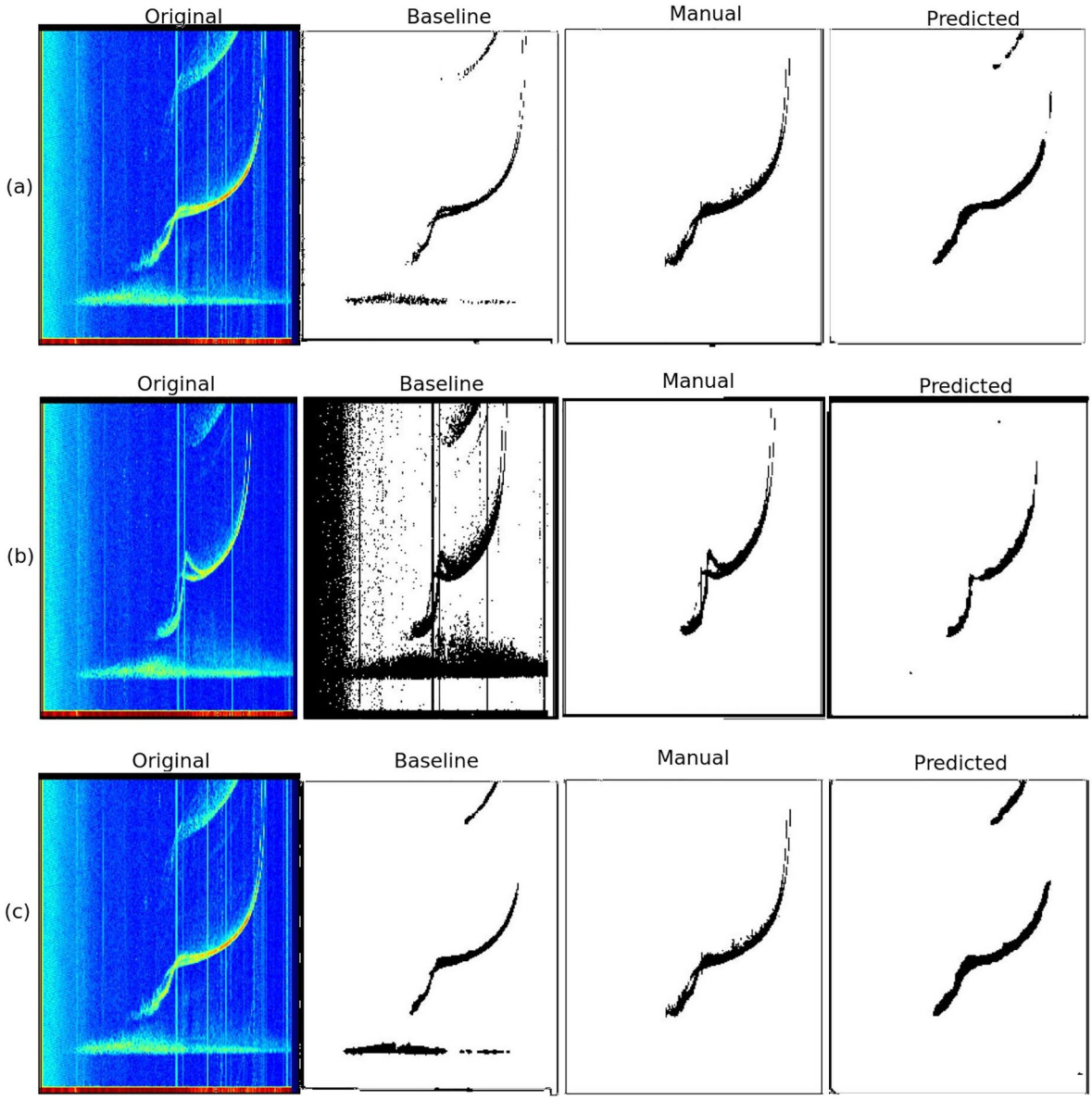

Figure 13. Fine-tuning and final prediction. (a) Kmeans, (b) Mean shift (c) filters.

6.2. Fine-Tuning: Using Manual Extraction to Improve Performance of CNN Models

In the second stage of the learning process, we fine-tune the previously trained models. The three models are fed again with original ionograms from the training/validation sets, but the output variables this time are ionograms with manually extracted traces from the training/validation sets, as shown in Figure 12.

Table 3
Fine-Tuned Convolutional Network Average IOU

	Filtered	K-means	Mean shift
IoU	0.589	0.602	0.593

Abbreviation: IoU, intersection over union.

Figure 13 shows the results of the different stages of the training process. Columns from left to right: Original ionogram, ionogram with traces extracted using a CNN trained with baseline models, manual trace extraction, ionogram with traces extracted using the CNN models plus fine-tuning. In the latter, it is observed that interference, background noise, calibration signal from the radar, and Es layer have been completely removed.

1944799x, 2021, 8, Downloaded from https://agupubs.onlinelibrary.wiley.com/doi/10.1029/2020RS007258 by Cochrane Peru, Wiley Online Library on [19/08/2025]. See the Terms and Conditions (https://onlinelibrary.wiley.com/terms-and-conditions) on Wiley Online Library for rules of use; OA articles are governed by the applicable Creative Commons License

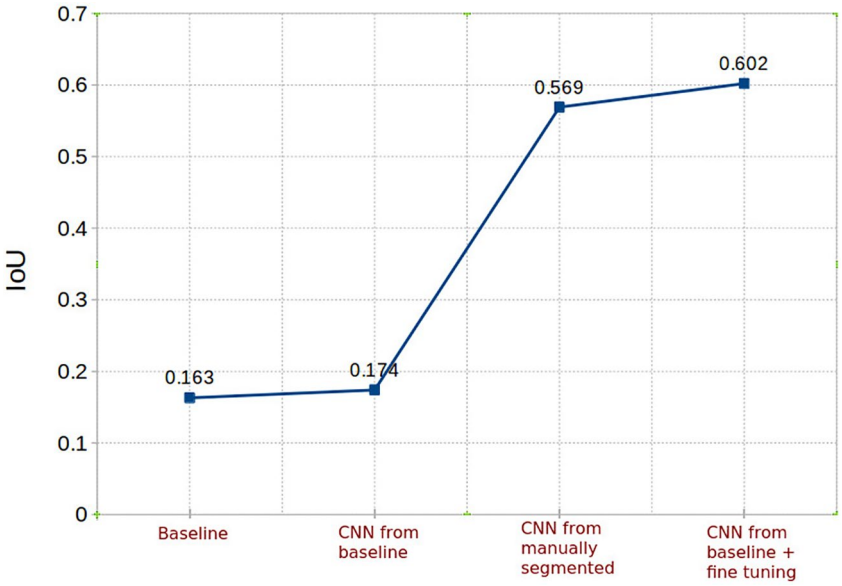

Figure 14. Average intersection over union of all models.

Average IoU between test set ionograms with traces extracted using fine-tuned models and manual extraction is summarized in Table 3. A significant improvement is observed compared with the IoU of trace extraction before applying fine-tuning.

6.3. Building a Neural Network Model From Labeled Ionograms Only

As a final stage, another CNN model was created using only manually extracted traces as training data, and no pretraining was used. This model gives an average IoU of 0.569, which is unexpectedly high given the small amount of data used for training.

Average IoU of all models are summarized in Figure 14.

Figure 15 shows examples of accurate predictions of unseen data (ionograms that do not belong to any of the sets used in the learning phase of the model development), showing good generalization performance.

Figure 16 shows inaccurate predictions on unseen data. This happens with ionograms that have weak traces, also with ionograms whose shapes have not been seen frequently during the training process. More manually scaled ionograms on a more diverse set of shapes should be created to reduce the number of inaccurate predictions.

7. Conclusions

1. In terms of IoU, trace extraction when using a neural network trained using labeled data is 5.6 times better than trace extracttion performed by baseline models.
2. The use of large amounts of unlabeled data to generate a pretrained model slightly improves (<6%) the accuracy of the final model, so we can say that performance of the model is based mainly on the use of labeled data for training and not on a pretraining process with unlabeled data.
3. In order to improve model generalization, it is necessary to train it with a greater amount of labeled data, from a more diverse set of ionograms, from different periods of time and geographic locations, covering a greater number of possible states of the ionosphere.

1944799x, 2021, 8, Downloaded from https://agupubs.onlinelibrary.wiley.com/doi/10.1029/2020RS007258 by Cochrane Peru, Wiley Online Library on [19/08/2025]. See the Terms and Conditions (https://onlinelibrary.wiley.com/terms-and-conditions) on Wiley Online Library for rules of use; OA articles are governed by the applicable Creative Commons License

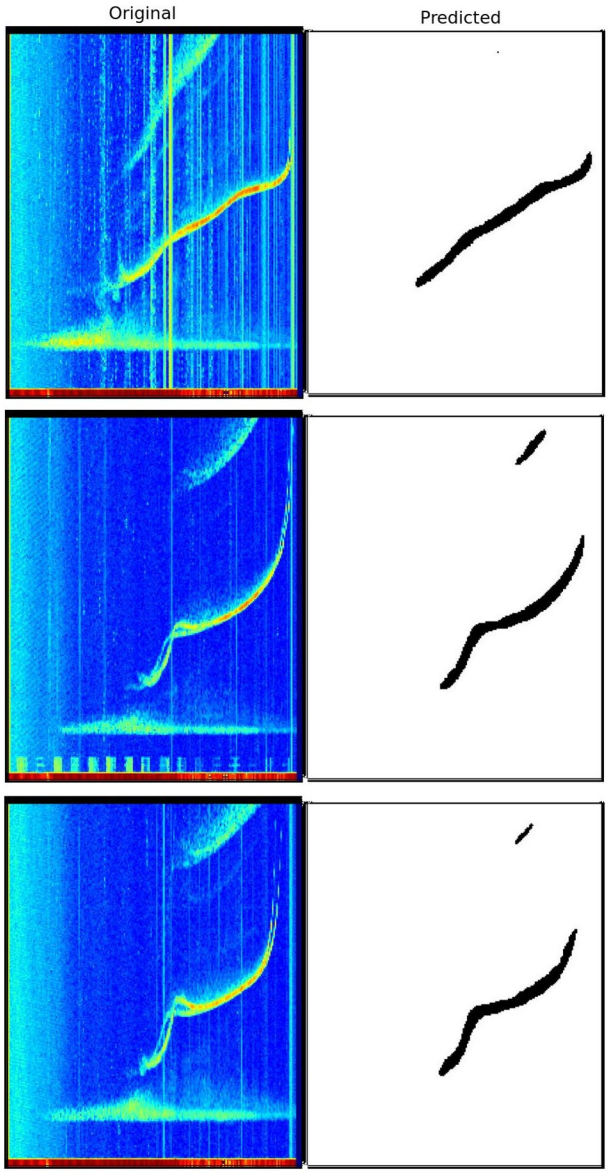

Figure 15. Accurate predictions of unseen data.

1944799x, 2021, 8, Downloaded from https://agupubs.onlinelibrary.wiley.com/doi/10.1029/2020RS007258 by Cochrane Peru, Wiley Online Library on [19/08/2025]. See the Terms and Conditions (https://onlinelibrary.wiley.com/terms-and-conditions) on Wiley Online Library for rules of use; OA articles are governed by the applicable Creative Commons License

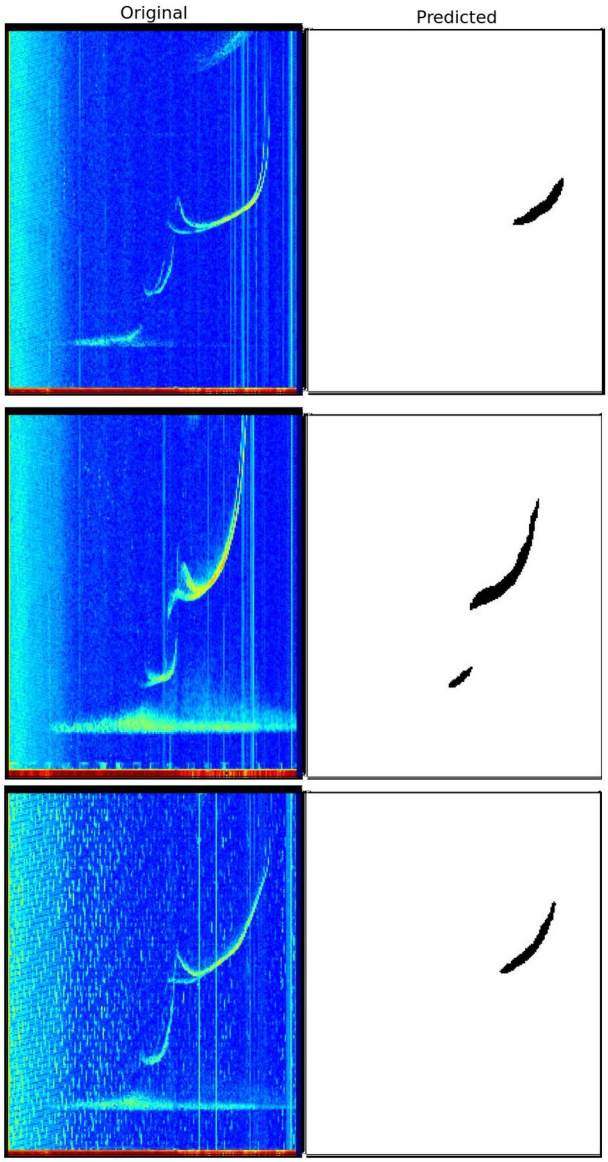

Figure 16. Inaccurate predictions of unseen data.

Data Availability Statement

Manually scaled ionograms can be downloaded from the public data set https://www.kaggle.com/cdelajara/ionograms under the names: manually segmented ionograms (png files) and models manualData lists-binary npz converted (npz files).

Acknowledgments
The Low Latitude Ionospheric Sensor Network (LISN) is funded by NSF Grant AGS-1933056 and is a project led by the University of Texas at Dallas in collaboration with the Geophysical Institute of Peru and other institutions that provide information in benefit of the space weather scientific community. The authors thank all organizations and persons that who support and operate receivers under the LISN project. All ionograms that were used to train the neural network models are available and can be downloaded from the following location https://lisn.igp.gob.pe.

References

Alexandre, B., Noelie, C., & Thibaut, C. (2018). *Ionospheric activity prediction using convolutional recurrent neural networks*. IEEE transactions on big data.

Bullet, T. (2015). *Software for reading VIPIR raw data files*. National Oceanics and Atmospheric Administration. Retrieved from ftp://ftp.ngdc.noaa.gov/

Chen, Z., Gong, Z., Zhang, F., & Fang, G. (2018). A new ionogram automatic scaling method. *Radio Science*, *53*(9), pp. 11149–81164. https://doi.org/10.1029/2018RS006574

Cheng, Y. (1995). Mean shift, mode seeking, and clustering. *IEEE Transactions on Pattern Analysis and Machine Intelligence*, *17*(8). https://doi.org/10.1109/34.400568

Ding, Z., Ning, B., Wan, W., & Liu, L. (2007). Automatic scaling of f2-layer parameters from ionograms based on the empirical orthogonal function (eof) analysis of ionospheric electron density. *Earth Planets and Space*, *59*(1), 51–58. https://doi.org/10.1186/BF03352022

1944799x, 2021, 8, Downloaded from https://agupubs.onlinelibrary.wiley.com/doi/10.1029/2020RS007258 by Cochrane Peru, Wiley Online Library on [19/08/2025]. See the Terms and Conditions (https://onlinelibrary.wiley.com/terms-and-conditions) on Wiley Online Library for rules of use; OA articles are governed by the applicable Creative Commons License

Galkin, I. A., & Reinisch, B. W. (2008). The new artist 5 for all digisondes. Ionosonde Network Advisory Group Bulletin, vol. 69, pp. 1–8.
Harris, T. J., Cervera, M. A., Pederick, L. H., & Quinn, A. D. (2017). Separation of o/x polarization modes on oblique ionospheric soundings. *Radio Science*, *52*(12), 1522–1533. https://doi.org/10.1002/2017RS006280
Harris, T. J., & Pederick, L. H. (2017). A robust automatic ionospheric o/x mode separation technique for vertical incidence sounders. *Radio Science*, *52*(12), 1534–1543. https://doi.org/10.1002/2017rs006279
Jursa, A. S. (1985). *Handbook of geophysics and the space environment*, Air Force Geophysics Lab Hanscom AFB MA.
lisn data user rules. Instituto Geofisico del Peru, 2019. Retrieved from http://lisn.igp.gob.pe/data/
Mochalov, V., & Mochalova, A. (2019). Extraction of ionosphere parameters in ionograms using deep learning. *E3S Web of Conferences*, *127*, 01004. https://doi.org/10.1051/e3sconf/201912701004
Network common data form netcdf. (2019) University Corporation for Atmospheric Research. Retrieved from https://www.unidata.ucar.edu/software/netcdf/
Observatorio distribuido lisn. (2019). Instituto Geofisico del Peru, Retrieved from http://lisn.igp.gob.pe
Perrone, L., Mikhailov, A., Cesaroni, C., Alfonsi, L., De Santis, A., Michael, P., & Scotto, C. (2017). Long-term variations of the upper atmosphere parameters on rome ionosonde observations and their interpreta- tion. *Space Weather and Space Climate*. *7*(A21).
Pezzopane, M., & Scotto, C. (2007). A method for automatic scaling of sporadic elayers from ionograms. *Radio Science*, *42*(2), RS2012. https://doi.org/10.1029/2006RS003461
Pezzopane, M., Scotto, C., & (2008). A method for automatic scaling of f1 critical frequencies from ionograms. *Radio Science*, *43*(2). https://doi.org/10.1029/2007RS003723
Pham, D., Dimov, S., & Nguyen, C. (1989–1996). Selection of k in k-means clustering. *Journal of Mechanical Engineering Science*, *203–210*. https://doi.org/10.1243/095440605X8298
Piggot, W., & Rawer, K. (1972). *URSI handbook of ionogram interpretation and reduction*. World Data Center for Solar-Terrestrial Physics.
Rahman, M. A., & Wang, Y. (2016). Optimizing intersection-over-union in deep neural networks for image segmentation. In *International symposium on visual computing*, (pp. 234–244). Springer. https://doi.org/10.1007/978-3-319-50835-1_22
Scotto, C., & Pezzopane, M. (2002). *A software for automatic scaling of fof2 and muf (3000) f2 from ionograms.*
Stankov, S. M., Jodogne, J.-C., Kutiev, I., Stegen, K., & Warnant, R. (2012). Evaluation of automatic ionogram scaling for use in real-time ionospheric density profile specification: Dourbes dgs-256/artist-4 performance. *Annals of Goephysics*, *55*(2). https://doi.org/10.4401/ag-4976
Valladares, C. E., & Chau, J. L. (2012). The low-latitude ionosphere sensor network: Initial results. *Radio Science*, *47*(4). https://doi.org/10.1029/2011rs004978
Xiao, Z., Wang, J., Li, J., Zhao, B., Hu, L., & Liu, L. (2020). Deep- learning for ionogram automatic scaling. *Advances in Space Research*, *66*(4), 942–950. https://doi.org/10.1016/j.asr.2020.05.009

1944799x, 2021, 8, Downloaded from https://agupubs.onlinelibrary.wiley.com/doi/10.1029/2020RS007258 by Cochrane Peru, Wiley Online Library on [19/08/2025]. See the Terms and Conditions (https://onlinelibrary.wiley.com/terms-and-conditions) on Wiley Online Library for rules of use; OA articles are governed by the applicable Creative Commons License